MASTER COPY KEEP THIS COPY FOR REPRODUCTION PURPOSES

REPORT DOCUMENTATION PAGE

Form Approved
OMB No 0704-0188

1. AGENCY USE ONLY (Leave blank)	2. REPORT DATE	3. REPORT TYPE AND DATES COVERED
	11/15/00	Final Report 10/16/95 - 3/16/00

4. TITLE AND SUBTITLE
High Power Mid-infrared Generation with a Quasi-Phasematched GaAs Guided-wave Optical Parametric Oscillator

5. FUNDING NUMBERS
DAAH04-96-1-0002

6. AUTHOR(S)
J. S. Harris and M. M. Fejer

7. PERFORMING ORGANIZATION NAME(S) AND ADDRESS(ES)
Stanford University
328 CISX 4075
Stanford, CA 94305

8. PERFORMING ORGANIZATION REPORT NUMBER

9. SPONSORING / MONITORING AGENCY NAME(S) AND ADDRESS(ES)
U.S. Army Research Office
P. O. Box 12211
Research Triangle Park, NC 27709-2211

10. SPONSORING / MONITORING AGENCY REPORT NUMBER
ARO 35005.3-PH

11. SUPPLEMENTARY NOTES
The views, opinions and/or findings contained in this report are those of the author(s) and should not be construed as an official Department of the Army position, policy, or decision, unless so designated by other documentation.

12a. DISTRIBUTION / AVAILABILITY STATEMENT
Approved for public release; distribution unlimited.

12b. DISTRIBUTION CODE

13. ABSTRACT (Maximum 200 words)
As described in our original proposal, the goal of this project is to create a new type of engineered nonlinear optical material, orientation-patterned GaAs, and use it to demonstrate improved high-power coherent mid-infrared sources. Consderable effort has been devoted over th- past decade to the development of mid-IR coherent sources based on nonlinear optical frequency conversion, e.g., optical parametric oscillators (OPOs), pumped by available high-power near-IR sources such as diode-laser-pumped solid-state lasers or near-IR diode lasers themselves. The rapid development of quasiphasematched materials, especially periodically-poled ferroelectrics, has revolutionized this field for wavelengths in the 2-4μm region. At 4 to 5 μm, absorption limits the maximum power attainable to the range of several watts, and operation is entirely precluded in the 8 to 12μm band. The orientation-patterned GaAs that we are developing is intended to complement periodically-poled ferroelectrics, providing a lithographically-engineerable low-loss material for high power devices at wavelengths beyond 4 μm.

14. SUBJECT TERMS

15. NUMBER OF PAGES
34

16. PRICE CODE

17. SECURITY CLASSIFICATION OF REPORT	18. SECURITY CLASSIFICATION OF THIS PAGE	19. SECURITY CLASSIFICATION OF ABSTRACT	20. LIMITATION OF ABSTRACT
UNCLASSIFIED	UNCLASSIFIED	UNCLASSIFIED	UL

High Power Mid-infrared Generation with a Quasi-phasematched GaAs Guided-wave Optical Parametric Oscillator

Final Progress Report

J. S. Harris
M. M. Fejer

October 16, 1995 - March 16, 2000

U. S. Army Research Office

DAAH04-96-1-0002

Stanford University

Approved for Public Release

Distribution Unlimited

Final Report

DAAH04-96-1-0002

High Power Mid-infrared Generation with a Quasi-phasematched GaAs Guided-wave Optical Parametric Oscillator

1. Introduction

As described in our original proposal, the goal of this project is to create a new type of engineered nonlinear optical material, orientation-patterned GaAs, and use it to demonstrate improved high-power coherent mid-infrared sources. Considerable effort has been devoted over the past decade to the development of mid-IR coherent sources based on nonlinear optical frequency conversion, e.g. optical parametric oscillators (OPOs), pumped by available high-power near-IR sources such as diode-laser-pumped solid-state lasers or near-IR diode lasers themselves. The rapid development of quasiphasematched materials, especially periodically-poled ferroelectrics, has revolutionized this field for wavelengths in the 2-4 μm region. At 4 to 5 μm, absorption limits the maximum power attainable to the range of several watts, and operation is entirely precluded in the 8 to 12 μm band. The orientation-patterned GaAs that we are developing is intended to complement periodically-poled ferroelectrics, providing a lithographically-engineerable low-loss material for high power devices at wavelengths beyond 4 μm.

Our most important accomplishment in this program has been the demonstration of all-epitaxial crystal inversion of GaAs thin films with respect to the underlying GaAs substrate, followed by the development of this technology to the point that it is now useful for fabrication of nonlinear optical devices. Prior to this accomplishment, most work in orientation-patterning semiconductors had relied on non-standard wafer bonding techniques,[1] while the attempts to fabricate such layers directly through epitaxy have produced less than desirable results due to problems with growth rate non-uniformities.[2] Our recently developed technique employs only a thin (30Å) nonpolar, lattice-matched Ge interlayer in an epitaxially grown GaAs/Ge/GaAs heterostructure. Two different GaAs crystal orientations of opposite polarity may nucleate on the nonpolar Ge layer. By introducing a misorientation to the GaAs substrate, we can break the symmetry of the Ge surface and preferentially nucleate one of the two possible GaAs domains, in particular that antiphase to the substrate. Subsequent processing and regrowth create an orientation-patterned GaAs template.[3] This "template" can be used as a substrate for the growth of diode-pumped thin-film waveguide optical parametric oscillator devices, the baseline approach of this program. Additionally and more importantly, thick film growth techniques such as Hydride

Vapor Phase Epitaxy (HVPE) can be used to grow very thick orientation-patterned GaAs films for use in bulk nonlinear optical parametric oscillator devices.

We report here results in material studies that helped refine the template fabrication technique, a detailed description of the template fabrication, waveguide device characterization, as well as what appeared along the way as a viable alternative to waveguide configuration: thick growth of OPGaAs films using hydride vapor phase epitaxy for bulk optics.

2. Antiphase growth studies

In order for the all-epitaxial approach to work, it is necessary to grow a layer of epitaxial GaAs on a thin Ge interlayer, such that the epitaxial GaAs is of the opposite phase, or rotated by 90°, compared to the original substrate. In addition, the GaAs must all be of the same phase across the surface of the wafer - any regions of opposite phase would negate any desired phasematching effects. Since the ability to grow high quality, antiphase GaAs was crucial to our approach, much work and time were spent investigating the necessary growth conditions. In addition to the direct applicability to the work presented here, it is hoped that this research will also be beneficial to other researchers studying polar-on-nonpolar epitaxy for other uses.

A. Background

Polar-on-nonpolar epitaxy has many potential applications and as such is widely studied. Heterojunction Bipolar Transistors (HBTs), using Ge as a base material, were widely studied because of the high hole mobility of Ge, and GaAs/Ge solar cells also have many useful properties.[4] By using materials of differing bandgaps to collect light from differing regions of the spectrum, the efficiency can be vastly improved. In addition, the ability to use Ge substrates, instead of more costly GaAs wafers, could have a substantial economic benefit, especially for space-based solar arrays. GaAs/Si heteroepitaxy, in the hopes of directly integrating GaAs optoelectronic devices with Si-based circuitry, encounters the same problems in addition to the lattice-mismatch (≈4%) problem. Using Ge_xSi_{1-x} as a buffer layer to accommodate the strain is one potential solution. Growth of GaP on Si has also been studied.[5]

As a result, there is a large body of literature - both theoretical and experimental - concerning polar-on-nonpolar epitaxy. In order to make suitable device grade material, two difficulties need to be overcome. First is the tendency of the polar material to form Antiphase Domains (APDs) and Antiphase Boundaries (APBs), when growth is nucleated on the nonpolar

material. Because of the higher symmetry of the nonpolar material (Ge) it is possible for two different phases of the polar material (GaAs) to nucleate on the nonpolar surface, so that growth may commence with either the cation plane or the anion plane. These regions of different phase are known as APDs, and are separated by APBs, as shown in Figure 1 by the dashed line.

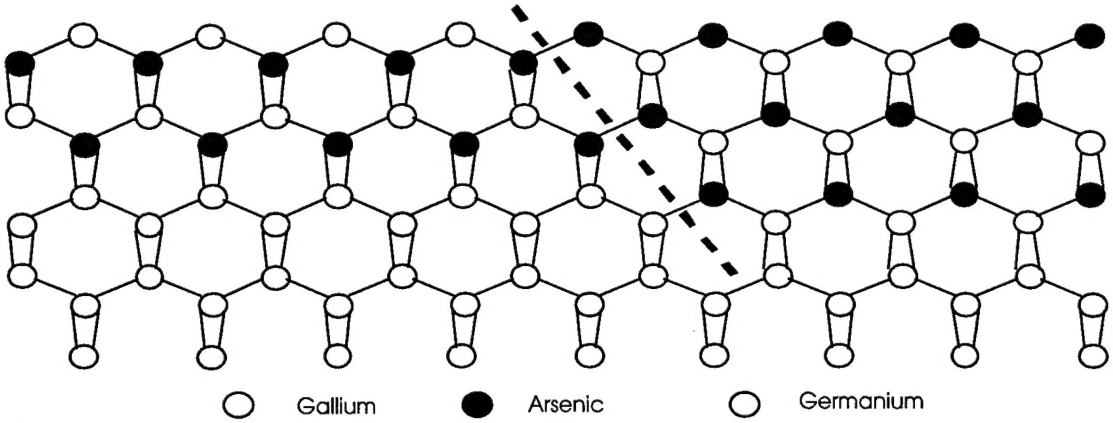

Figure 1: Antiphase Boundary (APB) and Antiphase Domains (APDs) resulting from a single step in the Ge surface.

Since the APBs consist of charged Ga-Ga or As-As bonds, their existence would degrade the performance of any electronic device. In addition, there is also the problem of cross-contamination resulting in unintentional doping between the two materials (i.e. Ge doping of GaAs). Since this second matter was not a concern for our ultimate (optical) devices, it will not be discussed in detail. Not surprisingly, it was found that APDs and APBs do indeed occur under standard growth conditions, most likely due to the occurrence of single steps in the nonpolar material, or incomplete prelayers. Calculations also showed that the nonpolar/polar interface must be nonplanar in order to avoid the buildup of significant electric fields.[6] Several researchers tried various surface treatments (high-temperature anneals, etc.) in order to promote the existence of double steps over single steps. Still other researchers tried growing on nonstandard crystal planes - such as (211) - in order to alleviate APDs.[7] It was observed that, instead of growing on a nominally flat (001) substrate, APD free material could be grown by using substrates with a deliberate misorientation introduced.[8] This result may be due either to the tendency of the misoriented wafers to form double steps, given the proper treatment, or to preferential bonding of one particular species of the polar material at the step edges, thus breaking the symmetry between the two. Based on the double-stepped model of APD-free growth, two essential conclusions can be reached. First, growth must be initiated with a monolayer of one species, as incomplete coverage will result in APDs. Second, the phase of the epilayer should be controlled by choosing which species to deposit first - i.e. a sample grown with an initial As monolayer should have the

opposite phase than one initiated with a Ga monolayer. One major difficulty with controlling the phase with the appropriate prelayer is avoiding As contamination of a Ga prelayer, since the chambers used for the growth of GaAs usually have a significant background pressure of As unless careful measures are taken. Any incomplete prelayer coverage can lead to a high APD density.

It was decided to use the results of Strite[910] et al. as a starting point towards growing antiphase GaAs, using a Ge interlayer. Their results indicated that single-domain GaAs could be grown on thin (~20 Å) Ge layers deposited on substrates misoriented 4° towards (111)A. In this particular instance, the epitaxial GaAs was the same phase as that of the substrate, as shown Figure 2(a). It can be seen that misorienting the GaAs wafer either towards (111)A or (111)B will result in the same misorientation (towards (111)) and step structure in the Ge epitaxial layer, due to its higher symmetry. If a wafer misoriented towards (111)B is chosen, however, the epitaxial GaAs will be antiphase to that of the substrate (Figure 2(b)).

This is exactly the effect that is desired. Another way of illustrating the matter is to consider the case of GaAs grown on Ge misoriented towards (111). Assume that the GaAs grows single-domain and with a fixed orientation with respect to the misorientation (i.e. the top GaAs is misoriented towards its (111)A plane). Then, by placing a misoriented GaAs substrate 'beneath' the Ge, we can create the GaAs/Ge/GaAs heterostructure. Since a substrate misoriented towards either (111)A or (111)B can be placed beneath the Ge misoriented towards (111), the top layer will either be in-phase or antiphase to the substrate, depending on which one is chosen.

Just by observing the misoriented Ge surface, however, it is not possible to see that a fixed orientation of GaAs will nucleate every time. That it does so was merely an observed experimental fact, reported by one research group. For our research to be successful, we would have to find the necessary growth conditions that would also allow us to grow APD free GaAs on thin Ge films. Then, by changing the misorientation direction by 90°, we should be able to grow antiphase films. We were mindful, however, of the results reported by other research groups so we also investigated a wide range of growth conditions and parameters, in order to expand our understanding of the process.

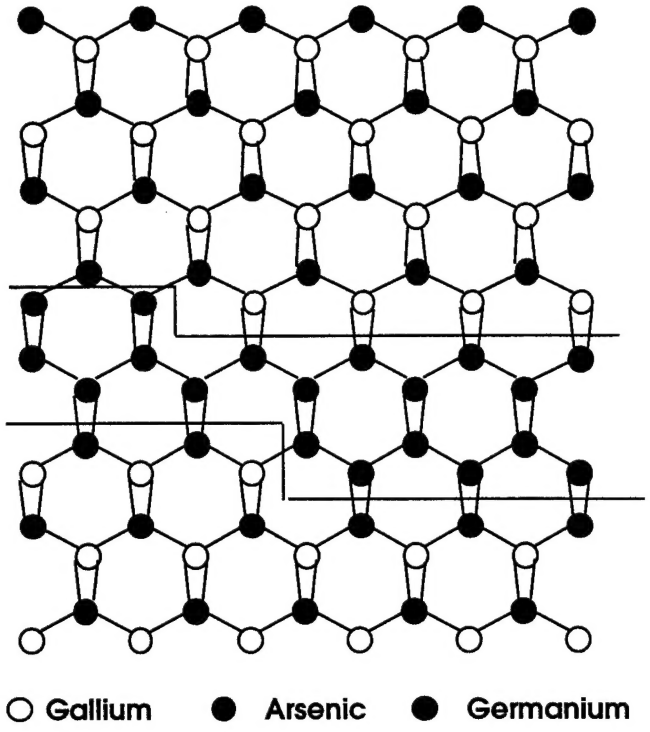

(a)

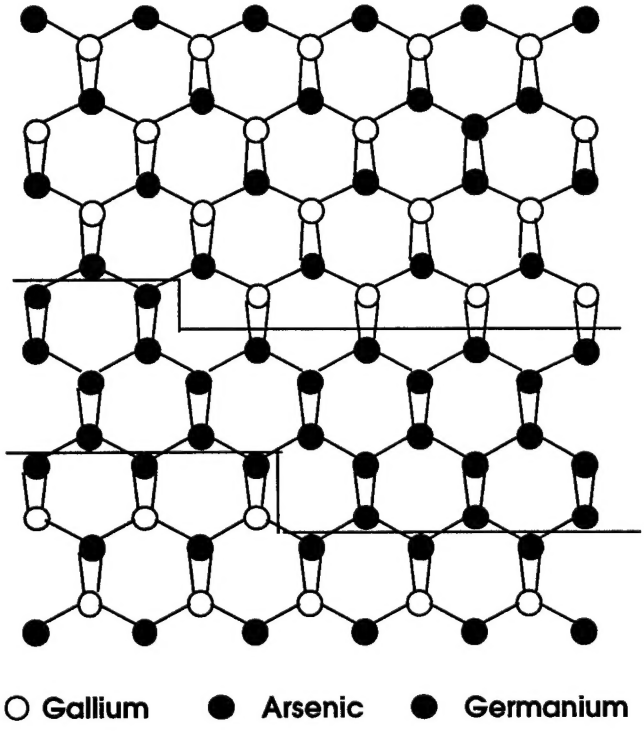

(b)

Figure 2: Schematic of growth of GaAs/Ge/GaAs heterostructures on surfaces misoriented towards (a) (111)A and (b) (111)B, following model of Strite et al.

B. Antiphase growth

Given the large number of variables that can affect the quality of epitaxial material, the parameter space to be investigated to discover the proper growth conditions was quite large. As explained earlier, the choice of misorientation was expected to determine the phase of the material, but this was not always the case. Most of the necessary work, therefore, went into attaining high quality, single-domain GaAs epitaxy on top of thin Ge layers. Depending on wafer availability, studies were done on substrates misoriented towards either (111)A or (111)B, with the expectation that the ability to grow single-phase material could be transferred between the two, with the choice of misorientation controlling the phase of the epilayer with respect to the substrate. Key variables studied include buffer layer structure, substrate temperature, and arsenic exposure during a high temperature Ge anneal step.

Feedback was provided mainly via optical inspection, RHEED, anisotropic etching, and SEM. As explained earlier, by using RHEED it is possible to distinguish between single-domain and mixed-domain material. In addition, it is possible to determine the orientation of the GaAs, relative to a misorientation direction. For the electron beam along the in-plane [110] direction, a 2-fold pattern will be seen, while a beam directed along the [1-10] direction will yield a 4-fold reconstruction, as shown in the first part of Figure 3. For single-domain GaAs grown on top of a Ge interlayer, 2-fold and 4-fold patterns will still be seen for proper orthogonal orientations of the electron beam, and will define the new [110] and [1-10] directions. If the GaAs epilayer [110] direction is parallel to the substrate [110] direction the material is in-phase, if the two directions are orthogonal then the GaAs epilayer is antiphase to the substrate. Some absolute reference is necessary to determine this, however, since it is impossible to simultaneously probe the substrate and GaAs epilayer using RHEED. One possibility is to 'zero' the degree counter of the substrate positioner along either the 2-fold or 4-fold pattern and compare this to the position of the GaAs epilayer 2-fold and 4-fold patterns; however errors in the stepper motor rotation, and hence the zero, may accumulate during long growths. If optical access is available to the growing wafer, the orientation of the RHEED beam compared to the major flat on the wafer can be used as a reference point. The easiest reference point, however, is the horizon due to the misorientation of the substrate. If the 4-fold pattern is seen above or below the horizon for the substrate and on the horizon for the GaAs epilayer, with the converse for the 2-fold pattern, then the GaAs epilayer is antiphase to the substrate. This is exactly the situation pictured in Figure 3.

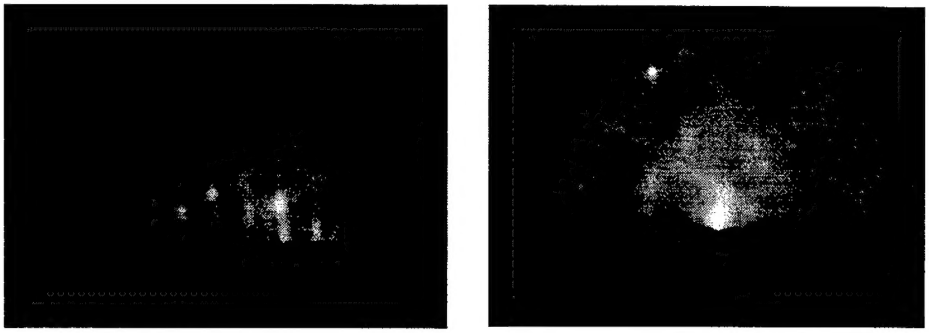

[110] [1$\bar{1}$0]

GaAs RHEED Patterns before Ge deposition

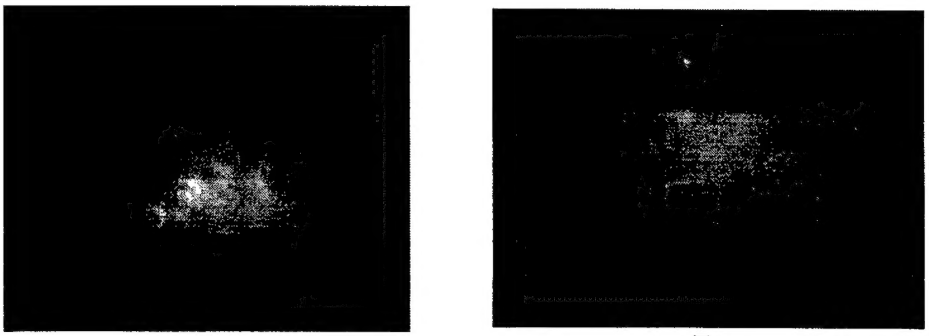

[110] [1$\bar{1}$0]

GaAs RHEED Patterns after Ge deposition and GaAs growth

Figure 3: RHEED pictures before and after Ge deposition, showing that the 2-fold and 4-fold patterns have switched directions.

Once the wafer is removed from the growth chamber, RHEED can no longer be used to probe the orientation of the film. In addition, the RHEED beam only probes a small spot of ~ $1mm^2$ near the center of the wafer. For *ex situ* measurements, and in order to characterize large areas, an anisotropic etching technique was developed. For the anisotropic etching, ridges were lithographically defined, along the [110] and [1-10] directions. The samples were then etched using a 1:1:6 $NH_4OH:H_2O_2:H_2O$, a preferential etchant that leaves the sidewalls either slanted along the {111} planes for ridges in the [1-10] direction, or slightly undercut for ridges in the [110] direction.

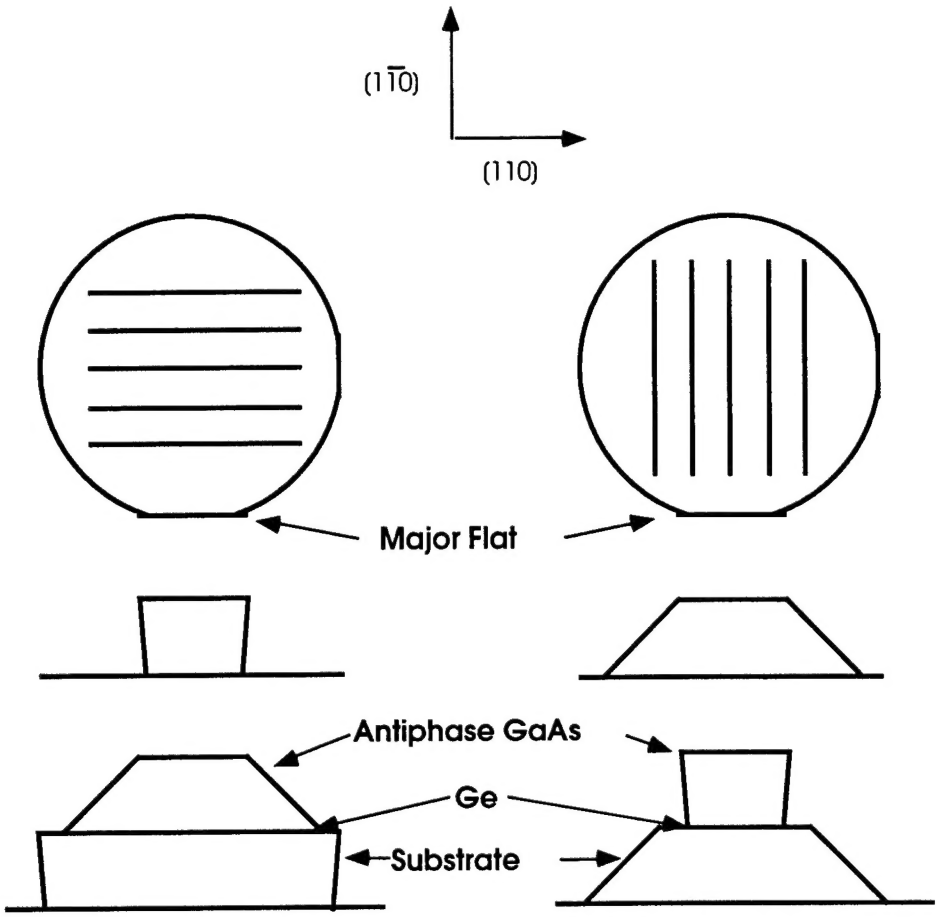

Figure 4: Etch profiles for features defined along in-plane [110] and [1-10] directions of a (001) wafer.

For antiphase GaAs epilayers, the sidewall profile will change as the etchant briefly stops and then goes through the Ge interlayer, while for in-phase material the sidewall angle will remain unchanged. For material with large numbers of APDs, severe disorder along the etching fronts could be detected under SEM examination, since a random mixture of V-groove and undercut etching would occur. A qualitative feel for the height of the APD propagation could also be obtained by comparing the heights of the disordered regions. Diagrams of the expected etch profiles are illustrated in Figure 4.

In order to test the necessary conditions for antiphase growth, the following test structure (Figure 5) was used, while varying only one parameter at a time. After growing a 1000 Å GaAs buffer layer via conventional MBE, a 100 Å Ge layer was deposited at 350° C. The Ge surface was then annealed for 15 min. at 640° C. Next, 10 ML of GaAs were deposited via the MEE technique, at nucleation temperatures ranging from 350° C to 500° C. Next, 1000 Å of GaAs were deposited via coevaporation at 500° C, after which the substrate temperature was raised to 620° C and another 9000 Å deposited.

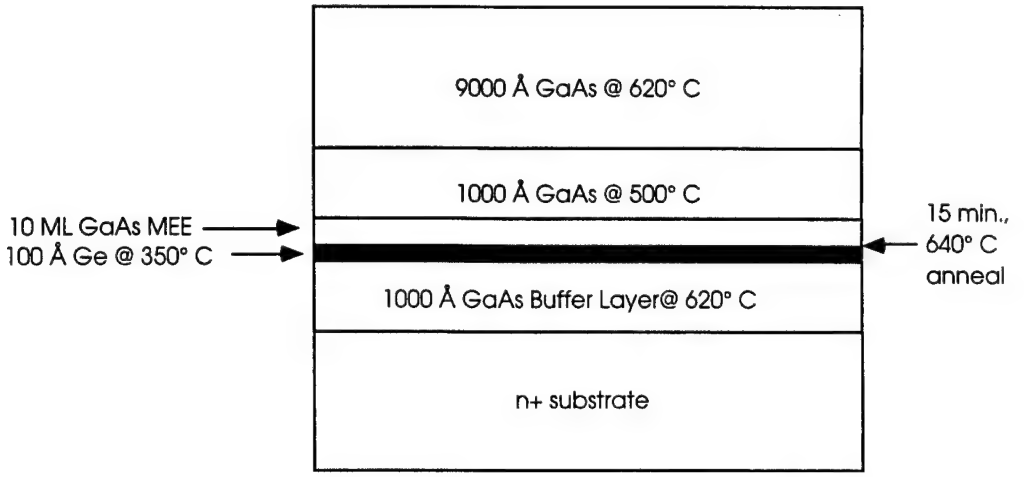

Figure 5: Schematic of test structure used for antiphase growth studies. Effect of nucleation temperature of the 10 ML MEE layer, substrate misorientation, and use of As during the anneal of the Ge surface were all studied.

Most of the materials characterization studies were done on substrates misoriented 4° towards (111)A, but samples were also grown on wafers misoriented 4° towards (111)B for comparison purposes. Samples were grown with and without an As_2 flux during the Ge anneal in order to study its effect on material phase. In addition, samples were grown with both As and Ga prelayers in order to discern any dependence there.

The first study done was to determine the effect of the MEE nucleation temperature on the phase of GaAs epilayer. Because our earlier studies had shown the tendency of a Ge film to roughen at high temperatures in the absence of As, an As_2 flux was supplied during the anneal. Using wafers misoriented towards (111)A, films nucleated at 350° C yielded material antiphase to the substrate (Figure 6), while films nucleated at 500° C yield material in phase with the substrate (Figure 7). It should be noted that this nucleation temperature refers only to the first 10 MLs of MEE on the Ge, the rest of the structures are identical. Furthermore, films grown on wafers misoriented towards (111)B show the expected opposite behavior - 350° C nucleation results in in-phase material, while 500° C nucleation results in antiphase material. In both cases, the epitaxial GaAs [1-10] direction is perpendicular to the misorientation-induced steps for low-temperature nucleation, while for high-temperature nucleation the [1-10] direction is parallel to the steps. No appreciable difference in material quality due to the difference in substrate misorientation was observed.

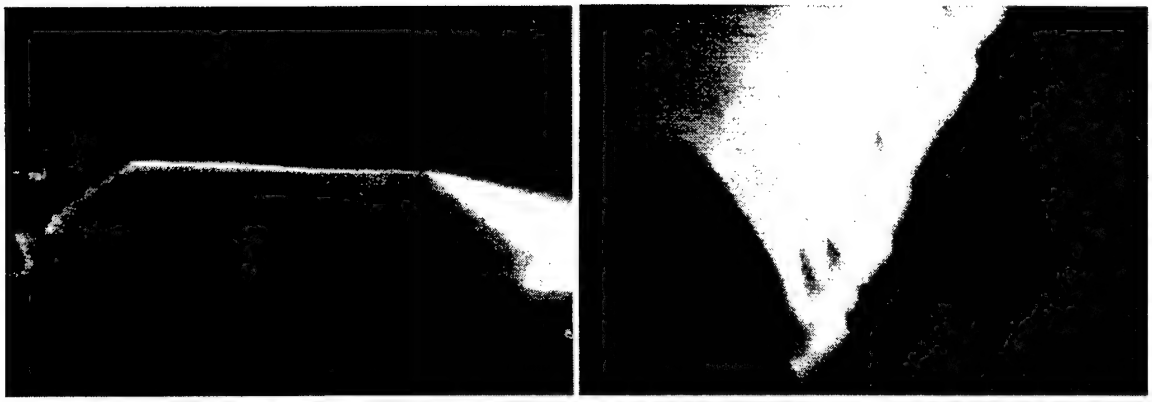

Figure 6: Cross section of film nucleated at 350° C, (a) showing epilayer GaAs antiphase to the substrate, and (b) showing smooth sidewall with small initial APD density. Substrate is (001) GaAs misoriented 4° towards (111)A.

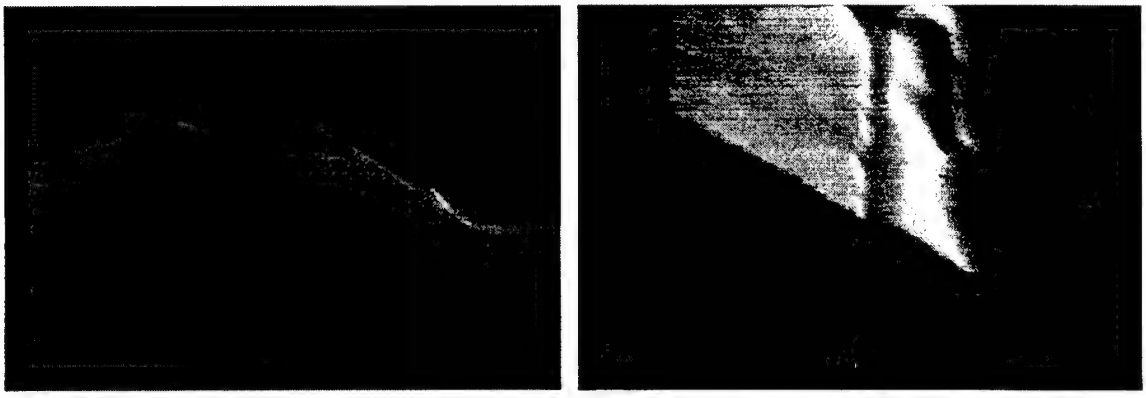

Figure 7: Cross-section of film nucleated at 500° C, showing (a) epilayer GaAs in-phase with substrate, and (b) smooth sidewalls indicative of low APD density. Substrate is (001) GaAs misoriented 4° towards (111)A.

The critical temperature appears to be at approximately 400° C, where the film becomes mixed domain. Optically, the surface appearance is quite cloudy, and preferential etching reveals evidence of a large density of APDs (Figure 8). It is important to compare samples etched for comparable amounts of time, as overetching in the preferential etch solution tends to exacerbate any defects in the material and give a false impression as to its quality.

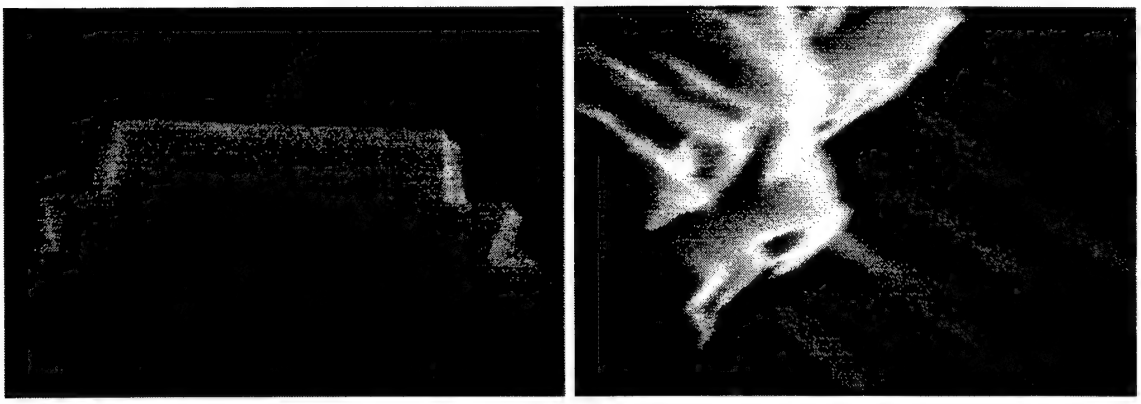

(a) (b)

Figure 8: Cross-section of film nucleated at 400° C, showing (a) poorly defined profile, and (b) high APD density. Substrate is (001) GaAs misoriented 4° towards (111)A.

By simply changing the nucleation temperature, it is possible to grow alternating layers of antiphase and in-phase material on the same substrate. Starting with a substrate misoriented towards (111)B, a thin Ge layer was deposited, followed by 10ML MEE GaAs at 500° C in order to grow antiphase material. After approximately 1 μm of GaAs growth, another Ge layer was deposited, and this time the 10 ML MEE GaAs were deposited at 350°C, because the antiphase material was now misoriented towards (111)A. The structure was then capped with 1 μm of GaAs. Photographs illustrating this double phase reversal are shown in Figure 9. Although such a structure might be useful for surface-emitting nonlinear optical devices, it cannot be used for normal-incidence interactions due to the symmetry of the $\chi^{(2)}_{xyz}$ tensor; however it does clearly illustrates the control over the GaAs phase for growth on a Ge surface.

Although our studies had shown a tendency of thin Ge layers to roughen during a high temperature anneal in the absence of a stabilizing As flux, the results of Sieg et al. were obtained by annealing without an As flux. Furthermore, an As flux had been reported to significantly change the nature of the Ge surface, making direct comparison of our results impossible with those of the other researchers.[11] Consequently, we decided to attempt growth on samples annealed in the absence of an As flux to see if high quality material could still be obtained, and if the same temperature dependences were observed.

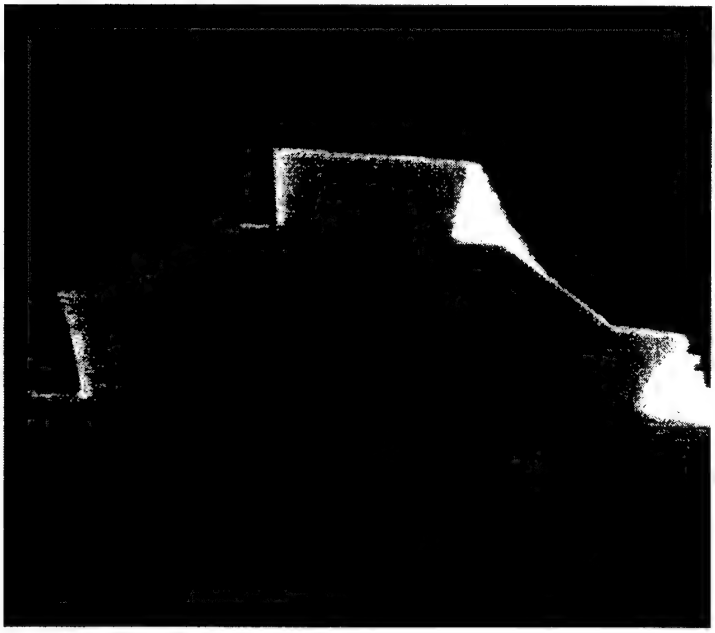

(a)

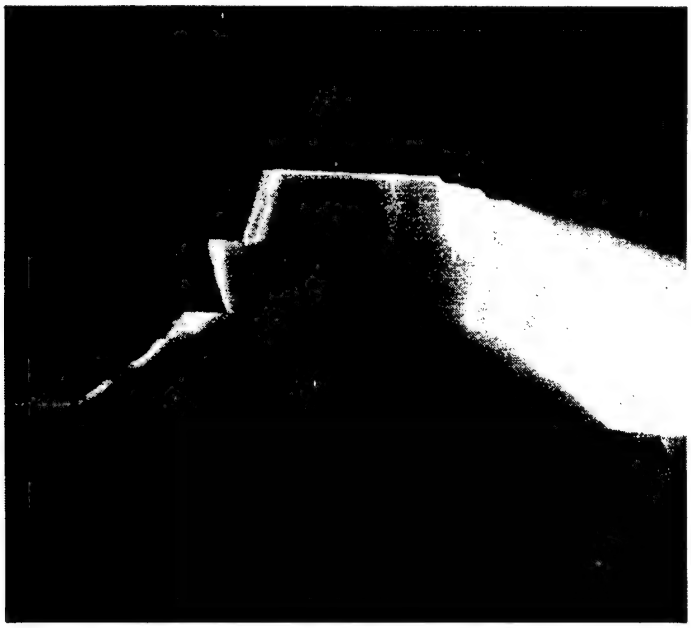

(b)

Figure 9: Cross-section views of samples containing layers of alternating phase. (a) is in the in-plane [110] direction, and (b) is in the in-plane [1-10] direction. Substrate is (001) GaAs misoriented 4° towards (111)B.

For growths with an As flux, the As valve and shutter were left open after the 640° C anneal had ended and until the substrate stabilized at the nucleation temperature. The valve and shutter were then closed and the first Ga layer of the 10 MEE cycles was deposited. For samples

annealed without an As flux, the first layer in the MEE cycle could be chosen to be either Ga or As, since the As valve and shutter were closed for approximately 40 minutes for the Ge growth and anneal. Four samples were grown without an As flux during the high temperature anneal (all on substrates misoriented towards (111)A): 1) Ga prelayer and 10 ML MEE GaAs at 350° C, 2) Ga prelayer and 10 ML MEE GaAs at 500° C, 3) As prelayer and 10 ML MEE GaAs at 350° C, and 4) As prelayer and 10ML MEE GaAs at 500° C.

For samples with a Ga prelayer, nucleation at both 350° C and 500° C resulted in epilayers which were in-phase with the substrate. It should be noted, however, that the film nucleated at 500° C had a high density of large APDs, as evidenced by preferential etching. Films nucleated with an As prelayer showed similar behavior to those annealed with As: 350° C nucleation resulted in growth misoriented towards (111)B, and 500° C nucleation resulted in growth misoriented towards (111)A.

Substrate Misorientation	As during Anneal?	Nucleation Temperature (C)	Prelayer	Phase
4° -> (111)A	Yes	350	---	-> (111)B (antiphase
4° -> (111)B	Yes	350	---	-> (111)B (in phase)
4° -> (111)A	Yes	397	---	mixed
4° -> (111)A	Yes	500	---	-> (111)A (in phase)
4° -> (111)B	Yes	500	---	-> (111)A (antiphase
4° -> (111)A	No	350	Ga	-> (111)A (in phase)
4° -> (111)A	No	500	Ga	-> (111)A (in phase)
4° -> (111)A	No	350	As	-> (111)B (antiphase
4° -> (111)A	No	500	As	-> (111)A (in phase)

Table 1: Growth conditions for various samples grown for antiphase growth studies.

C. Discussion

The temperature-dependence of the phase of GaAs growth on Ge has been observed and reported before while other researchers have observed dependence on either prelayer type (As vs. Ga) or As species (As_2 vs. As_4). Li et al. explained this phenomenon through competing mechanisms of terrace-dominated vs. step-dominated nucleation.[12] Nucleation occurs on both the steps and terraces simultaneously, but with competing domains. For high temperature growth (or large misorientation angle) the step-nucleated islands have time to coalesce, thus resulting in single-domain material. For lower temperatures (or smaller misorientation angle) the step-nucleated islands and terrace-nucleated islands do not have time to coalesce, thus the terrace-nuclei overgrow the step-nuclei, resulting in single-domain material that is of opposite phase compared

to that of the high temperature scenario. It should be noted that the second case always results in a nonzero APD density, while the first case can theoretically result in completely APD-free growth. According to their definitions, GaAs-B (with its [1-10] direction parallel to the steps) nucleates at low temperature, while GaAs-A (with its [1-10] direction perpendicular to the steps) is the high temperature phase. The GaAs-A phase nucleates at the steps edges due to the combination of Ge surface dimers running parallel to the step edges and an As layer used to initiate growth. GaAs-B nucleates on the terraces, following Kroemer's model for Ga-dominated growth while maintaining electric neutrality at the interface.[13] Our results are in direct contrast with those presented by Li et al., since we observe GaAs-A to be the low-temperature phase and GaAs-B to be the high-temperature phase. The use of MOCVD with its high H_2 concentration, as opposed to MBE, may explain this apparent contradiction, due to the different nature of the Ga precursors and temperature regimes of these two processes.

The effect, if any, of As during the 640° C anneal of the Ge surface is harder to ascertain. Since the two samples grown with As prelayers behaved identically to those grown with As during the anneal, the only effect of the anneal might be to insure an As prelayer. In contrast, the samples with Ga prelayers do not show the same temperature dependence as the other samples, with both the 350° C nucleation and the 500° C nucleation samples having the same phase. Two possible explanations can be proposed. One possibility is that in the absence of an As monolayer, the Ga mobility is high enough even at 350° C that the sample is growing in the step-nuclei regime instead of the terrace-nuclei. For either the As anneal or the As prelayer sample, there is enough As around to reduce the Ga mobility enough so that the terrace nuclei dominate. An alternative explanation would also assume that the high temperature (500° C) growths grow in the step-nuclei regime, due to the greater Ga mobility at that temperature. The difference between the low temperature (350° C) Ga and As prelayer samples would be due to the difference of the prelayer itself, as would be expected for a perfectly flat or double-stepped surface.

Through the above studies, we were able to determine the proper conditions for APD-free growth of material suitable for template formation. Two important conclusions were established that were necessary in order to fabricate orientation-patterned GaAs samples. First, it was learned that through the proper combination of substrate misorientation and nucleation temperature antiphase GaAs could be reliably grown on thin Ge interlayers. Second, it was determined that the phase is established by as little as 10 ML of growth on the Ge interlayer. Although a finite number of APDs may exist, they eventually grow out and the desired phase will dominate. Using

this second piece of knowledge, suitable templates could be designed using thin antiphase GaAs epilayers, instead of growing for several thousand Angstroms to insure APD-free films.

D. Template fabrication

A template optimized for regrowth should have a minimal (or no) corrugation, leave surfaces suitable for epitaxial regrowth, and involve a minimum of processing. Properly preparing the surface for regrowth and maintaining a minimal corrugation are often two contradictory goals, since traditional surface preparation techniques usually rely on backetching significant amounts of material, typically on the order of microns, in order to achieve a good surface.[14] Consequently, any initial corrugation on the order of several hundred Angstroms would be completely eliminated by such a step. In order to reproducibly fabricate a corrugation of known depth, it was decided to use a pair of AlGaAs etch stop layers, combined with selective etching, in order to selectively expose alternating phases of GaAs. Because initial results had indicated antiphase growth was only possible on wafers misoriented towards (111)B, these substrates were used for the growth of all template wafers due to a greater supply, even though subsequent investigation led to the possibility of using substrates misoriented towards (111)A as templates.

Early on during the growth experiments, it was noticed that epilayers grown on wafers misoriented towards (111)B had a cloudy or hazy final appearance, while the same structure grown on wafers misoriented towards (111)A would appear specular and mirror-like. This was due to the different nature of the growth mechanisms occurring on the two misorientations, as discussed earlier. For substrates misoriented towards (111)A, Ga bonds are left dangling, while substrates misoriented towards (111)B have As dangling bonds. Arsenic dangling bonds are more reactive, leading to finger-like growth projections. In contrast, step-flow growth occurs more readily for substrates misoriented towards (111)A, resulting in a smoother surface. Since the mechanisms for APD-free growth rely on a controllably-stepped surface, the roughening that occurs during growth on surfaces misoriented towards (111)B is extremely detrimental since it results in steps of varying types. In order to grow antiphase material on substrates misoriented towards (111)B, it was necessary to overcome this problem, and several different buffer layer designs were investigated.

The first attempts focused on depositing approximately 500 Å of GaAs by MEE in hopes of smoothing out the growth surface. In order for a lift-off technique to be viable, a buffer layer of only a few hundred Angstroms would have to suffice. Unfortunately, these thin MEE buffer layers were inadequate, resulting in the same hazy or cloudy appearance. Next a buffer layer

consisting of a GaAs/AlAs superlattice was employed, approximately 1 μm thick. AlAs/GaAs interfaces have a tendency to getter impurities, specifically oxygen, and it was hoped this would lead to a smoother growth front.[14] This was indeed the case, and this buffer layer was employed for subsequent growths of template structures on substrates misoriented towards (111)B. This buffer layer was also employed during the regrowth of the waveguide structures, for the same reasons.

A typical template consisted of the following structure (Figure 10):

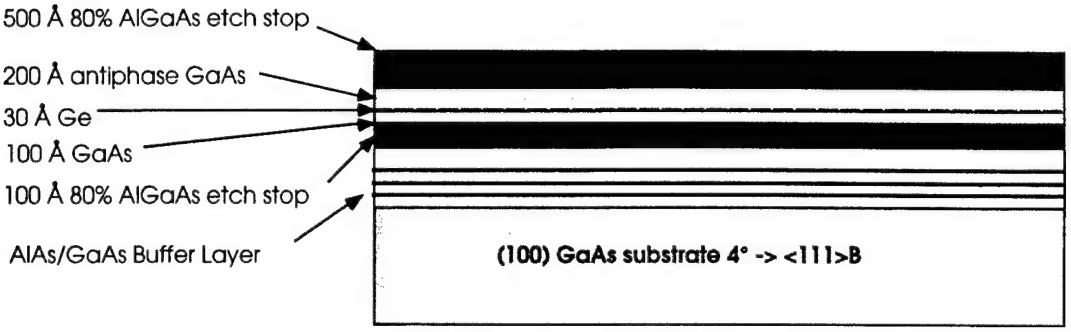

Figure 10: Schematic of template structure used for patterned regrowth.

The 1 μm buffer layer consisted of a 50Å AlAs/ 450Å GaAs superlattice (with three 500 Å AlAs marker layers inserted to help with SEM analysis). Since the substrate was misoriented 4° towards (111)B, the 200 Å GaAs layer on top of the Ge was deposited at 500° C, in order to achieve growth antiphase to the substrate. The 80% AlGaAs layers served as etch stops in order to selectively expose regions of alternating phase, as explained in the next section.

The templates were then lithographically patterned with the desired gratings, in order to quasi-phasematch the particular interaction of interest for that sample. A mask with several different grating lengths was used, in order to ensure the waveguide was phasematched in the available pump band. Typically the entire template wafer would go through the lithography step as one piece, after which it was quartered. One quarter was often used for calibration samples in order to accurately measure etch times, while the other three were processed for regrowth. Either whole, half, or quarter wafers were ideal for regrowth, as these shapes could easily be accommodated in our substrate holders by changing the inserts.

The use of selective etching and etch stop layers allowed for the reproducible fabrication of a specific, known, corrugation depth. A 1:1 $HCl:H_2O$ mixture was used to selectively etch only the 80% AlGaAs layers, and to stop on the GaAs layers. A mixture of 4:1 citric acid:H_2O_2

was then used to etch through GaAs and Ge layers, while stopping on the AlGaAs layers. Using these techniques, the depth of the corrugation was determined by the placement and thickness of the various layers.

The template was prepared for regrowth through the following steps (Figure 11):

1. Lithographically define the desired grating patterns on the substrate, using conventional techniques.

2. Pattern top etch stop layer with 1:1 HCl:H_20 (typically 30-45 s etching time), followed by a 5 minute running DI rinse.

2. Strip photoresist, 3-solvent clean (hot degreaser, acetone, and hot isopropanol), and O_2 plasma clean.

3. Pattern structure down to bottom etch stop layer using 4:1 citric acid:H_2O_2 (1:00 - 1:15 etching time), followed by a 10 minute running DI rinse.

4. Remove top and bottom etch stops simultaneously with 1:1 HCl:H_20 (1:00 etching time), followed by a 10 minute running DI rinse.

5. Blow dry and load into machine.

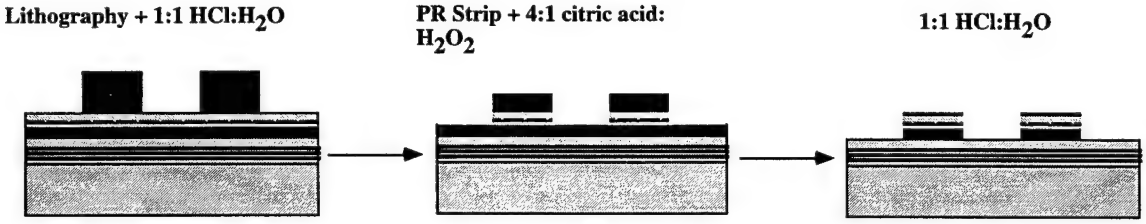

Figure 11: Etch sequence used to pattern templates.

Once again, the parameter space of variables to be investigated was quite large: etch stop thicknesses, etching times, final cleaning procedure, etc. Test samples were typically etched and measured with a profilometer in order to determine etching times. Equally important, however, was observing the color changes of the sample as the etch goes through the different layers, as this could be used to adjust the etching times as necessary on the larger pieces. Due to thin layers used, and the index contrast between GaAs and AlGaAs, these changes were quite noticeable as the sample color changed from dark blue to green to pink through the various processing steps. It was observed that it was necessary to overetch with the 1:1 HCl:H_2O mixture on the last step in order to assure good quality material in the subsequent MBE regrowth. In general, all of the steps

were overetched in order to ensure complete removal of the layer. Unfortunately, this leads to noticeable lateral etching, which decreased the duty cycle of the grating from the ideal 50%.

The above template structure (Figure 10) is not ideal, as it leaves a residual corrugation of over 400 Å. This could be reduced by decreasing the thickness of the layers, however some finite corrugation would still remain. This structure was chosen because of the well-characterized selective etching processes that could be employed using AlGaAs etch stop layers, and the ready availability of the necessary selective etches. In addition, the final HCl-based etch leaves a nice surface for regrowth, devoid of any oxide, after removing simultaneously the top and bottom etch stop layers. Thus, both regrowth surfaces remained protected from contamination until the final step. Logistically, the use of only two etches (and three total etching steps) simplified the process so the whole procedure could be done quickly to minimize any contamination before the wafer was reloaded into the MBE chambers.

As mentioned, the current template structure could be improved. Another, perhaps better, possibility would be to use a lift-off technique. For example, a dielectric layer is deposited on a misoriented substrate. The dielectric layer is then patterned with the appropriate grating periods, and the substrate is backetched to a depth of 500 - 1000 Å. After the appropriate cleaning, the wafer is loaded into the MBE system, where the appropriate buffer layer/Ge/antiphase GaAs structure can be grown on the exposed regions, with the dielectric layer serving as a growth mask. The sample is then removed from the machine and the dielectric layer lifted off, exposing alternating regions of antiphase and substrate-phase material. The desired structure can then be grown on the template. Ideally, the thickness of the buffer layer/Ge/antiphase GaAs structure will be equal to the depth of the backetching, so that no corrugation should result in the final template.

Once the template was patterned and reloaded into the MBE machine, it was necessary to find a set of growth conditions that resulted in high quality material suitable for waveguide devices. Issues to be considered include the quality of the surface after etching and regrowth preparation, growth on a corrugated sample, and the simultaneous growth on surfaces misoriented towards both (111)A and (111)B.

RHEED examination of the processed template, once inside the UHV growth chamber, showed little evidence of any oxide on the surface. Even so, the samples were annealed for 10 minutes at 700° C, under an As_2 flux, in order to remove any traces of oxide before growth. In an attempt to smooth out any initial corrugation and also to inhibit any Ge diffusion, the first 500 Å of the regrowth were deposited via the MEE technique. Due to the increased Ga mobility, it was

expected that the longer migration length would facilitate the filling in and smoothing out of the initial corrugation from the template. It was also necessary to remember that growth was occurring on surfaces misoriented towards both (111)A and (111)B simultaneously. As mentioned earlier, growth on surfaces misoriented towards (111)A is generally preferred, as the dangling bonds and step structure generally promote the step-flow regime of growth, in contrast to the finger-like growth found on substrates misoriented towards (111)B. Just as it was found necessary to grow an AlAs/GaAs superlattice buffer layer for the template growth, the same buffer layer structure was also employed during the waveguide regrowth and once again gave similar improvement. In both cases, this is probably in part due to the tendency of GaAs/AlAs superlattice to pin impurities and other crystal defects at the interfaces.

In order for successful devices to be realized, it was crucial that the intentionally formed antiphase boundaries (induced by the template) propagated vertically during subsequent growth of thicker layers. In other words, it was necessary for them to propagate along a vertical [110] direction. Other researchers, especially those utilizing MOCVD growth, had observed a tendency of the APD boundaries to propagate along {011} planes at a 45° angle to the (001) surface.[15] This would result in the domains closing over, which would nullify the desired QPM effects of such a structure. MBE growth, however, is much more kinetically driven than MOCVD growth, so the situation could indeed be quite different. Figure 12 shows a cross-section of an orientation-patterned film grown via MOCVD (using a wafer-bonded template), where closure of the domains can be seen.[1]

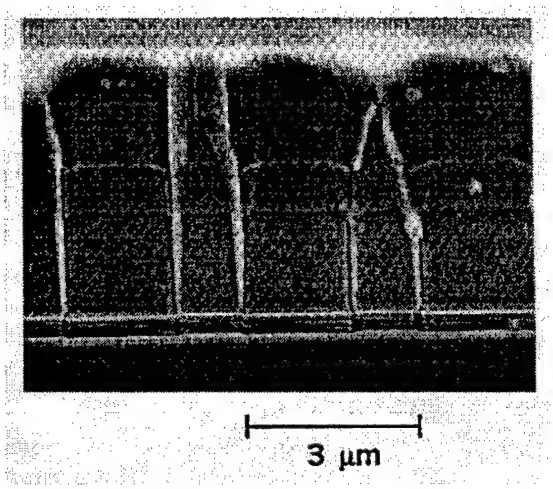

Figure 12: Cross-section of orientation-patterned GaAs film grown via MOCVD using a wafer-bonded template. Note the tendency of the domain boundaries to wander.[1]

On some of the first samples, thick (2-3 μm) GaAs layers were grown for characterization purposes, instead of AlGaAs waveguide structures. Stripes were than patterned perpendicular to the gratings, and the samples etched in the 1:1:6 $NH_4OH:H_2O_2:H_2O$ preferential etchant. Since regions of different domains should etch differently - with alternating slanted and undercut sidewalls (Figure 13), it was quite clear that indeed the template orientation was preserved on the surface, even after 2-3 μm of growth, and that the vertical propagation lines were not due to any residual effects from a corrugation.

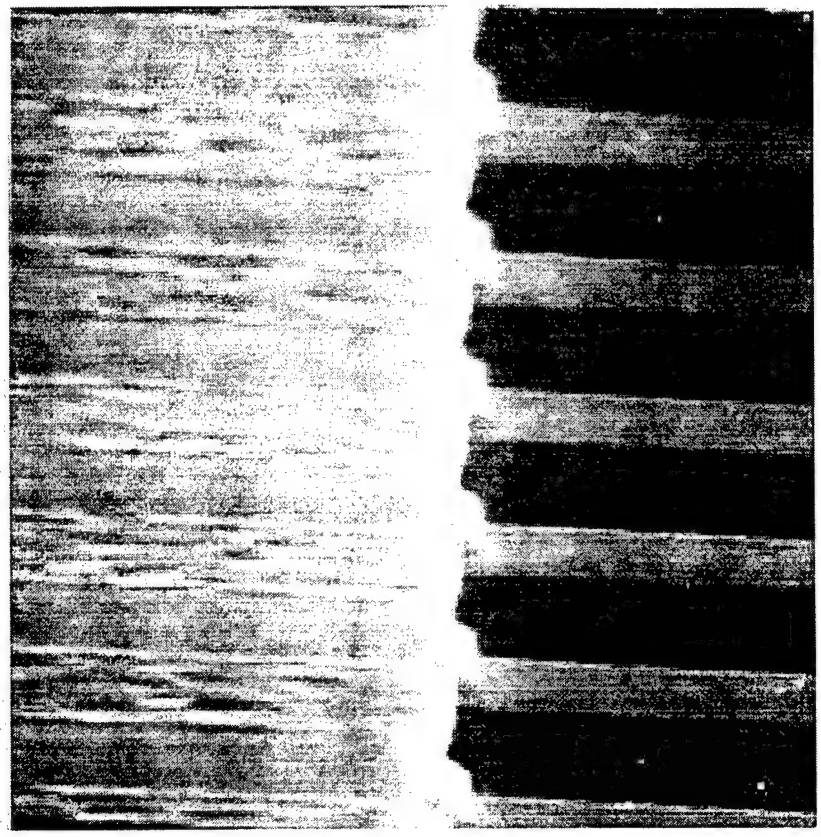

Figure 13: SEM micrograph of anisotropically etched orientation-patterned GaAs film, showing alternating regions of slanted and undercut sidewalls.

In conclusion, using our optimized parameters, we have now demonstrated the growth of mirror-smooth rotated GaAs thin films of sufficient quality for use as template substrates in the process outlined in Figure 11, with the quasiphasematching pattern set only by optical lithography.

3. Regrowth on orientation templates

Once template fabrication is completed, a regrowth step is necessary to obtain the desired structure for nonlinear optical interactions. In this section we describe the various steps we took during the course of this project and the evolution towards using thick film growth instead of the waveguide configuration for the mid-IR applications considered here.

A. MBE regrowth of quasiphasematched waveguides and optical results

Once fabricated using the method described above, an orientation template was then placed back into the MBE system for regrowth of orientation-patterned layers. A 1 μm thick GaAs/AlAs superlattice buffer was regrown first, followed by the desired waveguide structure. The superlattice buffer was required to prevent roughening of the regions tilted towards (111)B during regrowth. . The sample has been stain-etched in $K_3Fe(CN)_6$ /KOH to reveal the antiphase boundaries (APBs) which are not otherwise visible on the cleaved surface.

In films of this kind, we observe vertical antiphase boundary (APB) propagation under all the MBE growth conditions which we have investigated (Figure 14). This is very important, for if the domain boundaries propagate at an angle with respect to the growth direction, the domains would close over at some point after the initiation of epitaxial regrowth and leave a fully uniform domain film useless for quasiphasematching. We observe similarly vertical APB propagation under all the growth conditions we have investigated, with growth temperatures varying between 500°C - 650°C and compositions between GaAs and $Al_{0.6}Ga_{0.4}As$. We have observed domain aspect ratios up to 10:1 (5 μm high: 0.5 μm wide) in such MBE regrown films. Our observation of stable {110} APB propagation is consistent with theoretical predictions that the lowest energy APBs should lie in these planes,[16] as well as with experimental evidence that such behavior occurs during MOCVD growth.[15]

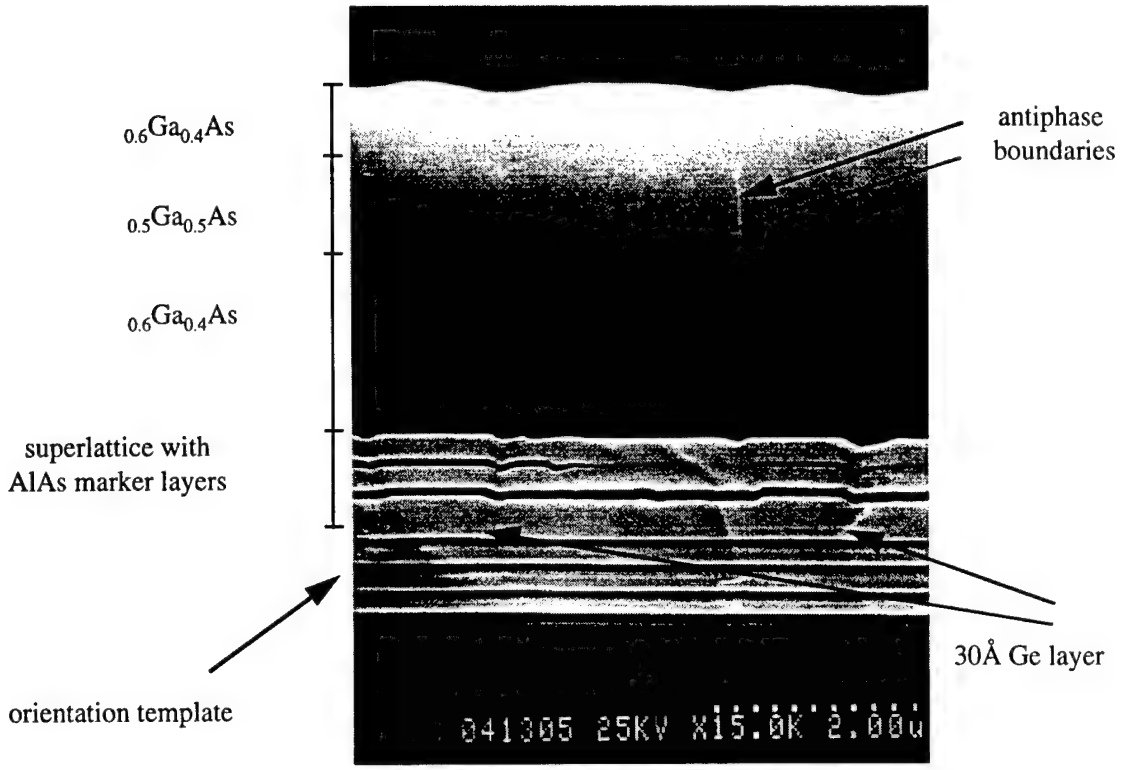

Figure 14: SEM micrograph of stain-etched cross-section of MBE regrown-waveguide layers on top of orientation template. Antiphase boundaries propagate vertically.

Ridge waveguides were produced using lithography and diffusion-limited wet chemical etching to pattern the top cladding layer. Figure 15 shows an SEM micrograph of the end-facet of the orientation-patterned waveguide. A small longitudinal corrugation is visible on the waveguide top surface disappearing along the guide due to the depth of field limitation of the SEM.

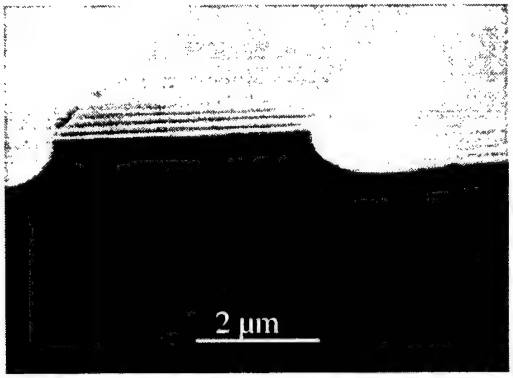

Fig 15: SEM micrograph of AlGaAs waveguide end-facet.

We then performed second harmonic generation in orientation-patterned ridge waveguides consisting of 2 μm $Al_{0.6}Ga_{0.4}As$ bottom cladding, 1 μm $Al_{0.5}Ga_{0.5}As$ core, and 1 μm $Al_{0.6}Ga_{0.4}As$ top cladding (structure shown in figure 14), in order to measure the conversion efficiency. Radiation from a tunable 1.55 μm external cavity diode laser was amplified in an erbium-doped fiber amplifier and end-fire coupled into the waveguide devices which had orientation gratings of length 0.84 mm. Figure 16 shows the normalized second harmonic generation efficiency as a function of fundamental wavelength in a device with a 3.75 μm orientation grating period.

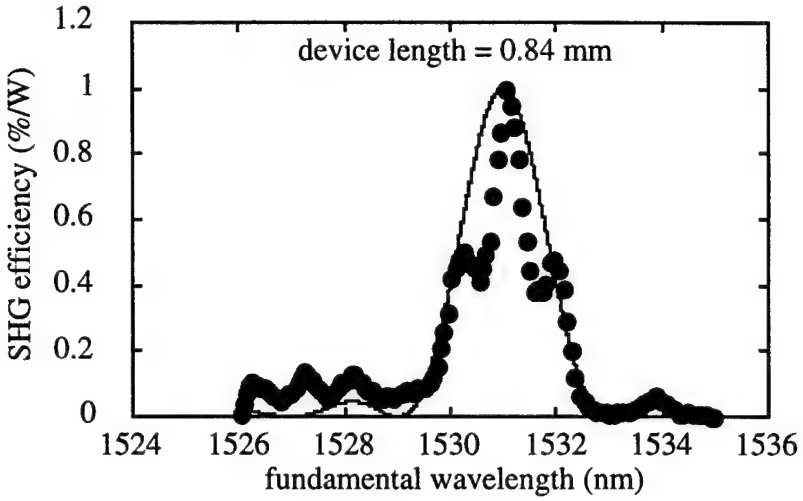

Figure 16: Tuning curve for second harmonic generation in orientation-patterned waveguide.

The maximum measured internal efficiency of this device is 1%/W, which should be compared to the calculated theoretical internal efficiency of 24 %/W for an ideal device without waveguide losses. We assumed d_{14} of GaAs to be 120pm/V. The measured FWHM bandwidth of the 0.84 mm long waveguide device matches the calculated value of 1.7 nm. The efficiency reduction from theoretical is caused by the large waveguide losses measured in these devices. Since these waveguides are single-moded around 1550 nm, we used the Fabry-Perot technique[17] and measured typical optical propagation losses around 40 dB/cm at 1550 nm in these devices. At 780 nm where the waveguides are multi-moded we measured waveguide losses using a variation on the cutback technique in which nominally identical waveguides with varying orientation-grating lengths are embedded in the same sample and found similar losses in the 40 dB/cm range. Interestingly, we observe similar losses in waveguides with and without orientation gratings on the sample, which leads us to conclude that the waveguide losses in devices fabricated

to date are dominated by complications with the epitaxial regrowth process which are unrelated to the orientation modulation. By comparing transmission in waveguides which had underlying Ge layers and waveguides which did not, we have ruled out free carrier absorption due to bulk Ge diffusion as a source of the high waveguide losses. We instead attribute the high waveguide losses to pinhole defects and other film nonuniformities that result from the un-optimized epitaxial regrowth process. We have subsequently determined that the regrowth preparation process used for these samples left a thin contamination layer across the template surface. In the hour following surface preparation, this contamination layer coalesced to form submicron size "blobs" in high density across the surface. Similar blob coalescence was observed on templates placed into the MBE system immediately after the preparation process. Investigation of the nominally regrowth ready sample surface using X-ray photoemission spectroscopy (XPS) indicated the presence of an aluminum and oxygen enriched layer. We have since modified the regrowth preparation process to include an additional brief H_2O_2 dip and final $HCl:H_2O_2$ dip before the DI rinse which eliminates this contamination. After the extra steps were included, we saw no blob growth on the surface and found no aluminum using XPS. As expected, the improved process gives much higher quality films with much lower pinhole defect densities. We anticipate that growth of new orientation-patterned films with this improved process will yield waveguide devices with much lower background waveguide losses, allowing investigation into the contribution of these orientation gratings to waveguide propagation loss. Since the blobs tended to coalesce on the edges of the template grating stripes where the APBs nucleate, we expect that this improvement should also improve the uniformity of regrowth at the APBs.

Before we determined the loss mechanisms in the quasiphasematched waveguides, we decided to evaluate the original design for OPOs using waveguide configurations. Figure 17 shows the threshold of a waveguide OPO versus loss in the waveguide. Considering the loss observed in our devices, we decided that it would be necessary to pursue other ways to build OPOs in quasiphasematched AlGaAs devices. For this reason, we started investigating the possibility of using thick growth techniques to fabricate bulk-like orientation-patterned AlGaAs crystals, so that we would not be limited by losses in waveguides. In the following section, we describe one such attempt using hydride vapor phase epitaxy (HVPE) as the thick film growth technique. However, studies of waveguide configurations are now again under way, in light of the improved fabrication process for our orientation templates.

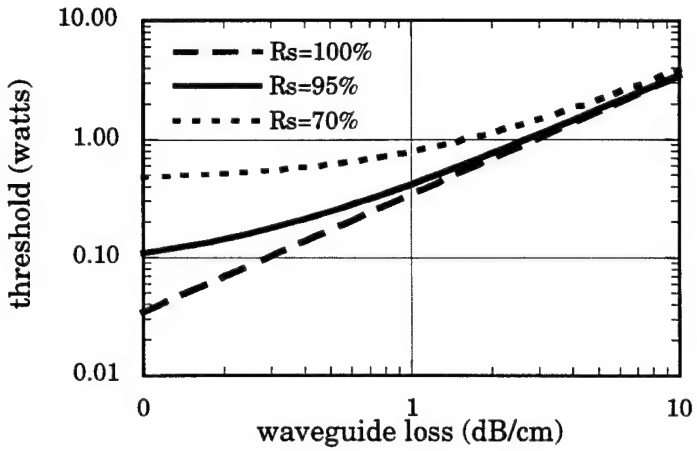

Figure 17: Calculated SRO threshold for GaAs/AlGaAs OPO as a function of waveguide loss.

B. HVPE thick growth on OPGaAs template

Following results by a group at Thomson-CSF about using HVPE regrowth on diffusion-bonded substrates showing vertical growth of antiphase domains in a thick GaAs films[18], we decided to collaborate with the French group and have them grow a thick film of GaAs on one of our templates.

The template was loaded into our MBE system for growth of a 5 μm GaAs seed layer for thick regrowth. Hydride vapor phase epitaxy (HVPE) growth was then performed using a conventional AsH_3/Ga+HCl/H_2 transport system. The hot-wall horizontal quartz reactor has two inlets, one for flow of HCl+H_2 over the 7N Ga source (providing gaseous GaCl) and the other for AsH_3, H_2 carrier flow and additional HCl. Total flow is about 1 slm. The temperatures of the Ga source and of the GaAs substrate were 850°C and 750°C respectively, and the growth occurred at atmospheric pressure. The vertical growth rate was about 20 μm/h. By varying the vapor phase composition (III/V ratio between 3 to 10), different stable lateral sidewall facets, either {011} or {111}, have been demonstrated in selective-area-masked stripe growth on (100) surfaces by HVPE.[19] For the present experiments we used growth conditions suitable for {011} sidewalls.

Figure 18 shows a cross-section of a 200-μm-thick orientation-patterned GaAs film. The cross-section has been polished and then stain-etched to reveal the antiphase domain boundaries (APBs), which were not visible after polishing alone. The domains are observed to propagate vertically through the 200μm thick HVPE film. Since we selected the grating stripes to run along

the direction of misorientation $[01\bar{1}]$ the APBs lie nominally in {011}. The fact that the duty cycle is unchanged with height indicates that APB propagation in {011} is stable under these HVPE growth conditions. For this reason it should be straightforward to grow OPGaAs films with thicknesses up to the $\geq$ 0.5 mm range and good domain quality. It is important to note, however, that APB propagation in {011} is not a general feature of GaAs growth on orientation templates under all growth conditions.

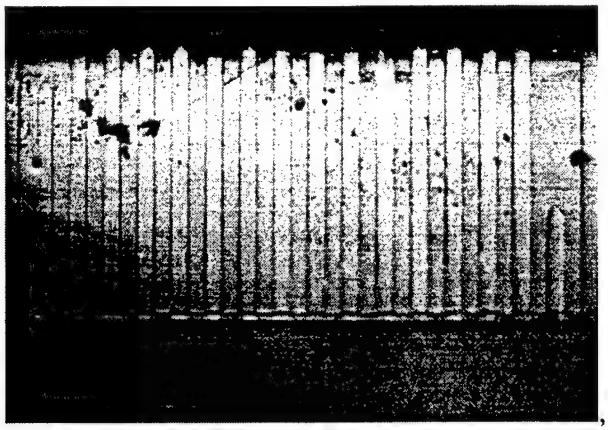

Figure 18: Stain-etched cross-section of 200μm thick orientation-patterned GaAs film with 27 μm grating period, illustrating vertical antiphase domain propagation under HVPE growth conditions.

A few of the domains in figure 18 close over abruptly after growing vertically for much of the film thickness. The uniformity of these domain interruptions in size and cross-section indicates an origin at the orientation template. Possible candidates for this nucleation problem include lithographic defects, oval defects in the MBE grown films, or some kind of dirt/contamination resulting from the wet processing. The 27 μm domain period demonstrated in these films is sufficient for first-order quasiphasematching of parametric interactions pumped at wavelengths of 1.5 μm and longer, making possible parametric oscillators and amplifiers generating radiation out to wavelengths beyond 12 μm using already available solid-state pump laser technology. So, with extension to thicker apertures, OPGaAs has the potential for enabling bulk frequency conversion throughout the mid-IR in a manner similar to what periodically-poled lithium niobate made possible at shorter wavelengths.

Figure 19: Stain-etched cross-section of 200μm thick orientation-patterned GaAs film with 212 μm grating period used for second harmonic generation with CO_2 laser.

Optical quality endfacets were polished on a 4.6 mm long piece of OPGaAs having the proper 212 μm domain period for quasiphasematching second harmonic generation of CO_2 laser radiation (Figure 19). The CO_2 laser source ran at a maximum power of 3 W CW and the beam was focused using BaF_2 lenses to a 50μm waist to make it approximately confocal in the OPGaAs crystal. Using the refractive index values of Pikhtin and Yaskov we can calculate the theoretical transmission including Fresnel reflections and multiple round trips to be 55.4%.[20] We measure a transmission of 50.6%. The difference is likely caused by clipping of the CO_2 beam at the corrugated top air/GaAs interface and in the highly doped substrate (n = 3e18) which exhibits large free carrier absorption at 10.5 μm.

For second harmonic generation, a sapphire plate was used to filter out the CO_2 radiation after the crystal before the 5.25 μm harmonic passed through a chopper and was detected using a pyroelectric detector. The 10.5 μm fundamental was polarized in the plane of the substrate, while the 5.25 μm harmonic was polarized orthogonal to that as required by the symmetry of d_{14}. Figure 20 shows the measured internal harmonic power as a function of CO_2 internal power at 10.5 μm with a clear parabolic dependence. Assuming a TEM_{00} gaussian fundamental beam, we calculate the effective nonlinear susceptibility (d_{eff}= d_{14}* 2/pi) in this film to be 48 pm/V as compared to the 57 pm/V we would expect with d_{14} = 90pm/V. Our reduced value of d_{eff} from theoretical likely results from the transverse mode quality of the laser, which we observed to be unstable and not consistently TEM_{00}.

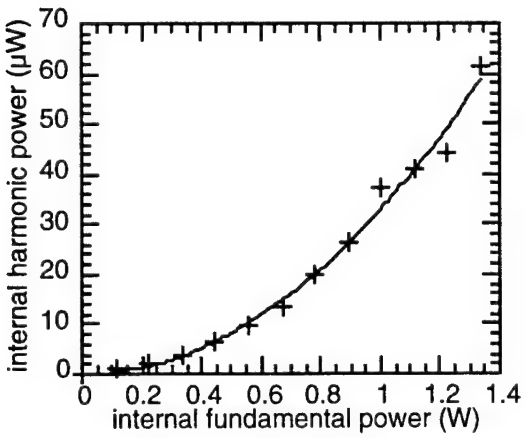

Figure 20: Internal harmonic power as function of internal 10.5 μm fundamental power for 212 μm period OPGaAs film.

Figure 21 shows the domain periods required for quasiphasematching various parametric nonlinear optical properties in bulk GaAs for various solid-state laser pump wavelengths. To date we have demonstrated excellent domain quality with periods down to 27 μm, which is sufficient for quasiphasematching any frequency conversion process pumped at wavelengths shorter than 1.55 μm. An additional factor of 2-3 reduction in the domain period, something which has been easily demonstrated in MBE-grown thin films, will allow pumping at 1.064 μm as well. The short periods (10s of μms) required for the near-IR pumps would be extremely difficult to fabricate by any other technique such as wafer bonding due to the difficulty of handling such thin fragile polished pieces of GaAs. Additionally, the wafer bonding technique scales poorly with these short periods, since ever more pieces are required just to fabricate the same overall length crystal. As a result, with the demonstrations we have done so far, we conclude that for OPO applications the orientation-patterned GaAs growth technique is superior to alternative techniques.

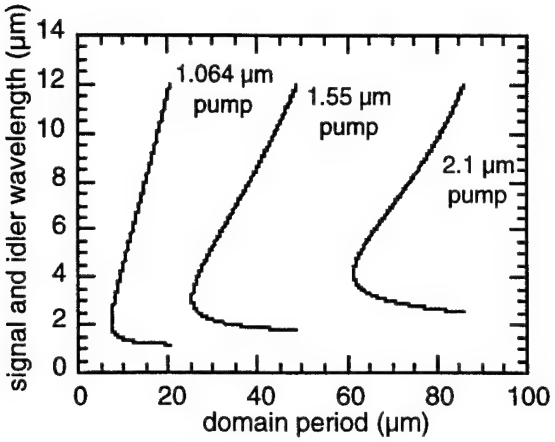

Figure 21: Domain periods required for quasiphasematching of various parametric interactions in orientation-patterned GaAs

4. SRO Modeling and projections/considerations

With the high waveguide losses measured in the orientation-patterned GaAs devices, combined with the breakthrough success in fabrication of thick orientation-patterned GaAs films, it makes sense to consider primarily bulk nonlinear optical devices for the near future. As discussed previously, the high waveguide propagation losses presently keep waveguide OPO thresholds out of the range of diode laser power levels. Therefore, we have examined the application of OPGaAs to bulk OPOs with near-IR pump lasers for generation of the mid-IR radiation sources proposed in the original proposal. One of the major advantages of GaAs for this application over the presently available chalcopyrite materials such as $ZnGeP_2$ and $AgGaSe_2$ is the possibility of pumping with well-developed near-IR lasers such as Nd:YAG and Yb:YAG, since the band edge of GaAs lies around 900 nm. Absorption in the near-IR region between the band edge and around 1.0 μm is dominated by the intrinsic Urbach tail to the bandedge absorption which results from phonon-induced broadening of the bands. After the Urbach tail falls off significantly, the absorption is dominated by extrinsic point defects such as dopants and anti-site defects. Typically, the absorption in commercial GaAs crystals is determined in the wavelength range of solid-state lasers by the high density of these point defects, leading to absorption in the 1 cm^{-1} range. This is unfortunately too high for fabrication of useful OPO devices, since the large absorption at the pump wavelength will necessarily lead to deleterious thermal effects in the OPO crystals. These effects hurt the OPO operation in two ways: first, thermal gradients in the crystal produce effective "thermal lenses" which distort the pump and signal beams, which raises

thresholds and decreases the OPO conversion efficiency. Second, thermal gradients also distort phasematching in the crystal, which effectively shortens the effective crystal length thereby similarly reducing both threshold and efficiency.

Our transmission measurements in OPGaAs show extremely low losses at 1.064 μm of 0.025 cm^{-1}. This level is more than an order of magnitude greater than the intrinsic limitation of the Urbach tail, but is dramatically lower than that achievable in bulk-grown GaAs crystals. This is not surprising, since the HVPE process has been demonstrated to produce films with doping levels < 10^{-14} cm^{-3}. At these absorption levels, pumping with 1.064 lasers is very feasible – for example, recent OPO devices utilizing $ZnGeP_2$ have successfully generated >10 Watt mid-IR output with absorption at the pump wavelength of 0.09 cm^{-1}.[21] This pump absorption level should be further reduced by more careful control over growth conditions and background doping levels, since the thick OPGaAs growths so far have not been optimized at all for such optical transmission but have only been used to investigate the domain propagation through thick films.

A second issue which will affect OPO operation is two photon absorption. At wavelengths shorter than half the band gap, there exists in GaAs an effective absorption which is proportional to pump intensity. In GaAs this half band-gap point lies around 1.7 μm wavelength. A plot of the GaAs TPA coefficient as a function of wavelength is shown in figure 22, where we can see that the coefficient drops from 23 cm/GW around 1.06 μm to 15 cm/GW at 1.55 μm.

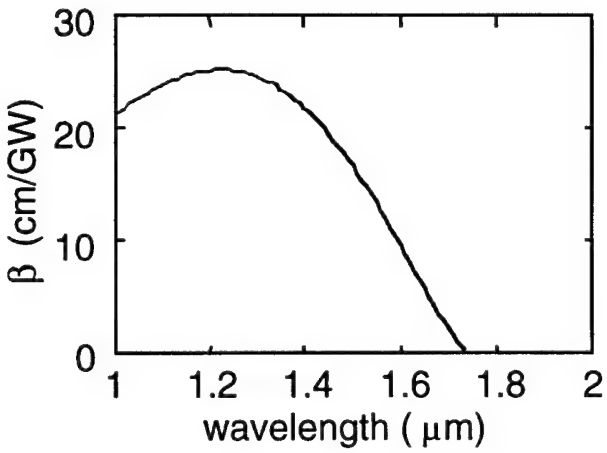

Figure 22: Two-photon absorption coefficient as a function of wavelength in GaAs

This additional absorption due to TPA can cause exactly the same deleterious thermal effects on beams and phasematching as the regular linear absorption losses. In designing an OPO using OPGaAs pumped at wavelengths < 1.7 μm, TPA must be taken into account. Moving to pump wavelengths > 1.7 μm eliminates all TPA-related effects. Unfortunately, many of the most

desirable pump lasers are around 1.0 μm, 1.3 μm, and 1.5 μm, which provides a motivation to determine whether there is a window of operation for such easily-pumped OPOs before TPA becomes a significant problem.

To determine the feasibility of short-wavelength-pumped OPOs, we have performed OPO threshold modeling using the approach of Byer, et al for pulsed OPOs.[22] Rather than make the approximations about pulse shape and gain made in the paper, we have elected to integrate the signal field in time through the temporal gain profile produced by the pump pulse. This method has the advantage of eliminating assumptions which break down as one moves into the longer pulse regime, while at the same time allowing simple incorporation of nonidealities affecting the pump pulse. In this model we have included the depletion of the pump pulse due to both linear and nonlinear (TPA) absorption through the crystal.

The modeled OPO is pumped at 1.064 μm and directly generates an 8.0 μm idler. The idler beam is set to be confocal in the OPGaAs crystal so that the idler beam will be of good beam quality. We utilize a ring cavity configuration to minimize extra signal attenuation which would result from another pass through the crystal. Figure 23 shows the threshold intensity as a function of crystal length and pump pulse length.

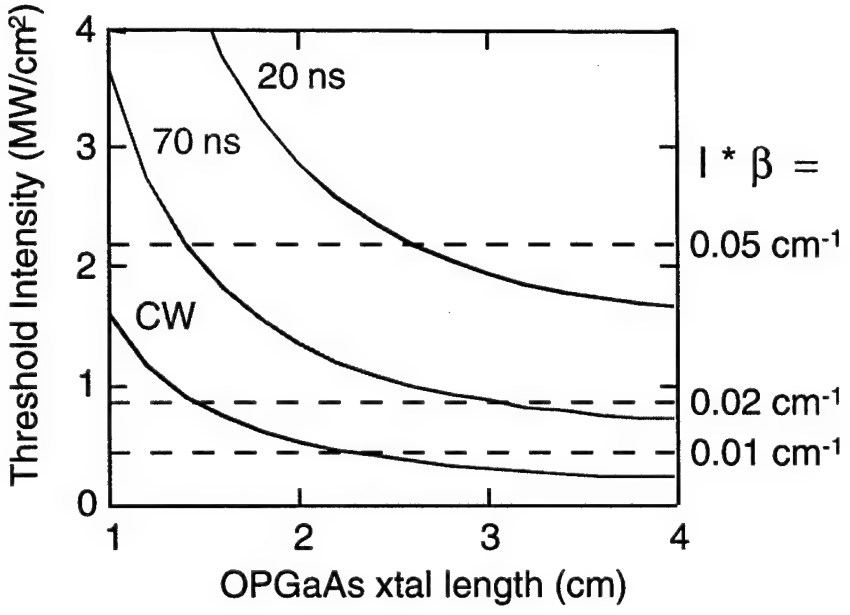

Figure 23: OPO threshold calculation for various configurations in bulk OPGaAs crystals

Intensity is plotted rather than energy since the most stringent limitation in this wavelength range will be the TPA, which is limited by pump intensity. On the right side of the graph is plotted the effective two photon absorption for the pump intensities shown on the left side. One sees immediately that it is critical to obtain crystals of at least 2 cm length to reduce threshold values down to point where the additional absorption due to TPA is lower than the already existing losses in the OPGaAs material. The reduction in threshold for longer pump pulse lengths results from having more passes through the gain medium to reach threshold and therefore permitting a lower single pass gain and associated pump intensity. Such as device might ideally be operated in a quasi-CW mode, which would minimize the pump intensities and the associated TPA while still delivering high average power operation. Taking the results with the 70 ns pump pulse and a 4 cm long OPGaAs crystal we obtain an energy threshold of 50 μJ. The pump intensities at this level are 50x below the damage threshold, leaving a significant window to pump the OPO without risking damage to the OPGaAs crystal. The damage threshold of OPGaAs is comparable to those of the chalcopyrite competitors, somewhere around 50 MW/cm^2 for nanosecond pulses. As usual, the damage threshold depends strongly upon the pulse length relative to the thermal relaxation time of the material. By moving to longer pulses in a quasi-CW device the thermal relaxation of the crystal would help dissipate the heat from absorbed pump radiation before it caused damage to the crystal.

From this study, we conclude that such mid-IR OPOs are a viable possibility in these new GaAs materials. More work needs to be done to determine the practical limits of their performance.

5. Conclusion

During the course of this project, our biggest accomplishment has been the demonstration of an all-epitaxial GaAs orientation-patterned template. This is the building block that many other groups had been looking for that will enable the kinds of devices that this project aims to fabricate. We have now developed a very reliable and reproducible process for growing these high quality templates.

We have shown that we can regrow low-loss material that conserves the orientation pattern, be it either in thin films or thick films. Domain boundaries propagate vertically throughout the films with no change in duty cycle or period length. We have been able to grow films with periods down to a few microns in waveguide devices, enough to phasematch any

interactions in the transparency range of AlGaAs, and down to 27 μm in thick HVPE films, enough to phasematch a 1.55 μm pumped OPO. These results are extremely promising, and work is underway in both waveguide devices and thick films to improve their characteristics and build useful frequency conversion devices. We have also demonstrated the first nonlinear optical results in all-epitaxial quasiphasematched AlGaAs devices. More materials research is needed to better understand the antiphase growth and the vertical propagation of domain walls, as well as to improve the quality of thick HVPE regrown films. Being able to grow thicker films, in the mm range, will allow GaAs devices comparable to what has been achieved in $LiNbO_3$, but in a different wavelength range.

In conclusion, we believe that our all-epitaxial orientation template technology, along with the demonstrated ability to grow films that conserve antiphase domains, will allow the development of many different frequency conversion devices, including for instance mid-IR high power quasiphasematched OPOs in thick films for countermeasure applications, as well as lower power applications in waveguide devices.

---

[1] S.J.B. Yoo, R. Bhat, C. Caneau and M.A. Koza, "Quasi-phase-matched second-harmonic generation in AlGaAs waveguides with periodic domain inversion achieved by wafer bonding," *Appl. Phys. Lett.*, **66**, p. 3410 (1995).

[2] M. J. Angell, R. M. Emerson, J. L. Hoyt, J. F. Gibbons, L. A. Eyres, M. L. Bortz, and M. M. Fejer, "Growth of alternating (100)/(111)-oriented II-VI regions for quasi-phase-matched nonlinear optical devices on GaAs substrates", *Appl. Phys. Lett.*, **64**, p.3107 (1994).

[3] C.B. Ebert, L.A Eyres, M.M. Fejer, and J.S. Harris Jr., "MBE growth of antiphase GaAs films using GaAs/Ge/GaAs heteroepitaxy", *J. Cryst. Growth*, **201-202,** p. 187 (1999).

[4] R. Fischer, W.T. Masselink, J. Klem, T. Henderson, T.C. McGlinn, M.V. Klein and H. Morkoç, "Growth and properties of GaAs/AlGaAs on nonpolar substrates using molecular beam epitaxy," *J. Appl. Phys.*, **58**, p. 374 (1985).

[5] S.L. Wright, H. Kroemer and M. Inada, "Molecular beam epitaxial growth of GaP on Si," *J. Appl. Phys.*, **55**, p. 2916 (1984).

[6] W.A. Harrison, E.A. Kraut, J.R. Waldrop and R.W. Grant, "Polar Heterojunction Interfaces," *Phys. Rev. B*, **18**, p. 4402 (1978).

[7] P.N. Uppal and H. Kroemer, "Molecular beam epitaxial growth of GaAs on Si(211)," *J. Appl. Phys.*, **58**, p. 2195 (1985).

[8] W.T. Masselink, T. Henderson, J. Klem, R. Fischer, P. Pearah and H. Morkoç, "Optical Properties of GaAs on (100) Si using molecular beam epitaxy," *Appl. Phys. Lett.*, **45**, p. 1309 (1984).

[9] S. Strite, D. Biswas, N.S. Kumar, M. Fadkin and H. Morkoç, "Antiphase domain free growth of GaAs on Ge in GaAs/Ge/GaAs heterostructures," *Appl. Phys. Lett.*, **56**, p. 244 (1990).

[10] S. Strite, M.S. Ünlü, K. Adami, G.-B. Gao, A. Agarwal, A. Rockett, H. Morkoç, D. Li, Y. Nakamura and N. Otsuka, "GaAs/Ge/GaAs heterostructures by molecular beam epitaxy," *J. Vac. Sci. Technol. B.*, **8**, p. 1131 (1990).

[11] P.R. Pukite and P.I. Cohen, "Suppresion of antiphase domains in the growth of GaAs on Ge(100) by molecular beam epitaxy," *J. Cryst. Growth*, **81**, p. 214 (1987).

[12] Y. Li, L. Lazzarini, L.G. Giling and G. Salviati, "On the sublattice location of GaAs grown on Ge," *J. Appl. Phys.*, **76**, p. 5748 (1994).

[13] H. Kroemer, "Polar-on-nonpolar epitaxy," *J. Cryst. Growth*, **81**, p. 193 (1987).

[14] E.C. Larkins and J.S. Harris, "Molecular beam epitaxy of high-quality GaAs and AlGaAs," in *Molecular Beam Epitaxy: Applications to Key Materials*, edited by R. F. C. Farrow (Noyes Publications, Park Ridge, N.J., 1995), p. 114.

[15] Y. Li and L.J. Giling, "A closer study on the self-annihilation of antiphase boundaries in GaAs epilayers," *J. Crystal Growth*, **163**, p. 203 (1996).

[16] P.M. Petroff, "Nucleation and growth of GaAs on Ge and the structure of antiphase boundaries", *J. Vac. Sci. Technol. B*, **4**(4), p. 874 (1986).

[17] R. Regener and W. Sohler, "Loss in low finesse Ti:$LiNbO_3$ optical waveguide resonators", *App. Phys. B*, **B36**(3), p. 143 (1985).

[18] L. Becouarn, B. Gerard, M. Brevignon, J. Lehoux, Y. Gourdel, and E. Lallier, "Second harmonic generation of a CO_2 laser using quasi-phase-matched GaAs layer grown by hybride vapor phase epitaxy", *Technical digest, CLEO 99*, p. 288 (1999)

[19] E. Gil-Lafon, J. Napierala, D. Castelluci, A. Pimpinelli, B. Gerard, and D. Pribat, "Kinetic modeling of the selective epitaxy of GaAs on patterned substrates by HVPE. Application to the conformal growth of low defect density GaAs layers on Si", *Proc. Materials Research Society*, **535**, D2.2 (1998)

[20] A.N. Pikhtin and A.D Yas'kov, "Dispersion of the refractive index of semiconductors with diamond and zinc-blende structures", *Soviet Physics - Semiconductors*, **12**(6), p. 622 (1978)

[21] P. A. Budni, L. A. Pomeranz, M. L. Lemons, P. G. Schunemann, T. M. Pollak, and E. P. Chicklis, "10W mid-IR holmium pumped $ZnGeP_2$ OPO", *OSA TOPS vol. 19 ASSL 1998,* p. 226 (1998)

[22] S. J. Brosnan and R. L. Byer, "Optical parametric oscillator threshold and linewidth studies," *IEEE J. Quantum Electron.* **QE-15**, p. 415 (1979)

Publications

L. A. Eyres, C. B. Ebert, H. C. Chui, J. S. Harris, Jr., and M. M. Fejer, "Fabrication of GaAs Orientation Template Substrates for Quasi-Phasematched Guided-Wave Nonlinear Optics", *Nonlinear Guided Waves and Their Applications*, **6**, 1995 OSA Technical Digest Series (Optical Society of America, Washington DC, 1995), pp. 156-158.

L. A. Eyres, C. B. Ebert, M. M. Fejer, J. S. Harris, Jr , "MBE growth of laterally antiphase-patterned GaAs films using thin Ge layers for waveguide mixing," Technical Digest Conference on Lasers and Electro-Optics Conference 1998, p. 276.

C. B. Ebert, L. A. Eyres, M. M. Fejer, J. S. Harris, Jr., "MBE growth of antiphase GaAs films using GaAs/Ge/GaAs heteroepitaxy" *J. Crystal Growth*, **202** pp. 187-193, May 1999.

Participating Scientific Personnel

C. B. Ebert, Ph.D., Stanford University, "Quasi-phasematched Waveguides for Infrared Nonlinear Optics Using GaAs/Ge/GaAs Heteroepitaxy," 1998.

L. A. Eyres, Research Assistant

T. J. Pinguet, Research Assistant

Inventions

Name of Inventor(s):	L. Eyres, M. Fejer, C. Ebert and J. Harris
Title of Invention(s):	Method for Fabricating Orientation-Patterned Gallium Arsenide Seeding Structures
Patent or Disclosure Number:	09/394,122